Pergamon

Int. J. Heat Mass Transfer. Vol. 37, No. 17, pp. 2661–2673, 1994

0017–9310/94 $7.00+0.00

0017–9310(94)E0101–Y

An analysis of subcooled turbulent film boiling on a moving isothermal surface

J. FILIPOVIC, R. VISKANTA† and F. P. INCROPERA

Heat Transfer Laboratory, School of Mechanical Engineering, Purdue University, West Lafayette, IN 47907, U.S.A.

(*Received* 7 *June* 1993 *and in final form* 15 *March* 1994)

Abstract—When film boiling occurs on a moving superheated surface, the vapor layer which forms between the surface and liquid reduces the drag force and heat transfer. In this study, heat transfer associated with subcooled turbulent film boiling on a moving isothermal surface is investigated using both local similarity and integral methods. Using a two-phase boundary-layer model and assuming power-law profiles for the velocity and temperature distributions, integral forms of the mass, momentum and energy-conservation equations, together with compatibility conditions at the vapor–liquid interface, were solved for both the vapor and liquid layers. In order to assess the merit of this analytical procedure, a local similarity solution to the same problem was obtained using the modified Cebeci–Smith eddy-viscosity model with the Cebeci–Bradshaw algorithm for turbulent boundary-layer flow. Numerical results reveal the effects of relevant parameters such as plate velocity, the ratio of plate-to-free-stream velocity, and liquid subcooling.

INTRODUCTION

WHEN film boiling occurs on a moving superheated surface, as is often the case in many engineering applications, the vapor layer which forms between the surface and liquid reduces the drag force and heat transfer, thereby acting as both a lubricant and insulator. In such applications, knowledge of forced film boiling flow and heat transfer is essential to the design and evaluation of related devices and processes. Representative applications include quenching in high-temperature materials prosessing [1], nuclear reactor safety [2] and drag reduction [3, 4]. Depending on the specific application, forced film boiling is achieved by effecting liquid flow over a stationary or moving superheated surface, or by moving a superheated surface relative to a liquid stream. In steel quenching processes, for example, moving strips or plates are cooled by liquid jets which impinge on the surface and divide into two streams, one of which moves in the same direction as the plate and the other in the opposite direction. Due to very high surface temperatures, both laminar and turbulent film boiling may occur.

The first studies of heat transfer in forced film boiling concerned circular cylinders [5, 6]. In subsequent studies, a two-phase boundary-layer model was used to compute laminar film boiling for flow over a horizontal plate under saturated [7] and subcooled [8] conditions. The results were confirmed by Ito and Nishikawa [9] and Nakayama and Koyama [10] who used numerical and integral methods, respectively, to solve the vapor and liquid boundary-layer equations.

The method proposed by Chappidi *et al.* [11] was an attempt to circumvent solving the full set of boundary-layer equations. Applying an analogy between conditions at the vapor–liquid interface and a surface moving in a single-phase fluid and using previously developed expressions for single-phase flow over a moving surface, they obtained good agreement between their approximate solution and numerical results based on solving the full set of governing equations for subcooled film boiling. However, agreement was restricted to film boiling under saturated conditions.

Zumbrunnen *et al.* [12] applied an integral method to obtain heat transfer results for laminar film boiling from a moving surface. They found that surface motion significantly increased heat transfer for subcooled, as well as saturated, liquids. Filipovic *et al.* [13] modified the model of Zumbrunnen *et al.* [12] to include conditions for which the surface moves through a quiescent fluid. In addition, numerical results obtained using a similarity solution for laminar film boiling over a moving surface were in excellent agreement with those of Zumbrunnen *et al.* [12].

In contrast to the numerous studies of laminar film boiling on a horizontal surface, little has been done to treat the problem of turbulent film boiling. The first such attempt [4] assumed the vapor layer to be a thin viscous sublayer in turbulent liquid flow, and an integral method was used to obtain skin friction and heat transfer results. Linear and 1/7-th power-law profiles were assumed for the vapor and liquid layers, respectively, and the empirical Blasius friction formula was applied at the vapor–liquid interface. The interfacial velocity was assumed to be independent of the x coordinate.

† Author to whom correspondence should be addressed.

NOMENCLATURE

A_j constant in equation (35)
Ar Archimedes number defined by equation (57)
a $m/(m+1)$
B constant in equation (46)
b $1+\varepsilon_m^+$
C_j constant defined by equation (35)
c $(1-m)/(m+1)$
c_p specific heat at constant pressure [J kg^{-1} K^{-1}]
D_1 $(2\bar{v}_p+n_v\bar{u}_s)$
D_2 $(2\bar{u}_s+n_l\bar{u}_\infty)$
d $1/(m+1)$
f dimensionless stream function defined by equation (11)
g gravitational acceleration [m s^{-2}]
h heat transfer coefficient [W m^{-2} K^{-1}]
h_c convective heat transfer coefficient in the presence of radiation across vapor layer
h_{co} convective heat transfer coefficient without radiation
h_R radiation heat transfer coefficient
h_T total heat transfer coefficient, h_c+h_R
h_1 size of the first $\Delta\eta$ step
h_{fg} latent heat of vaporization [J kg^{-1}]
I quantity defined by equation (37)
Ja Jakob number, $c_{pv}(T_p-T_s)/h_{fg}$
K the ratio of successive $\Delta\eta$ steps
k thermal conductivity [W m^{-1} K^{-1}]
L_{cr} critical wavelength of two-dimensional instability [m]
m constant defined by equation (36)
Nu_x local Nusselt number, hx/k_v
n exponent in equations (28), (29), (30) and (31)
Pr Prandtl number, $\mu c_p/k$
Pr_t turbulent Prandtl number, $\varepsilon_m/\varepsilon_h$
p exponent in equations (40) and (41)
q'' heat flux [W m^{-2}]
r $1/Pr+\varepsilon_m^+/Pr_t$
Re_x local Reynolds number, $u_i x/\nu_l$
Re_{δ_v} Reynolds number of the vapor film, $U_v\delta_v/\nu_v$
T temperature [K]
U_l $|u_\infty-u_s|$ [m s^{-1}]
U_v $|u_s-v_p|$ [m s^{-1}]
$\bar{U}_l$ U_l/u_i
$\bar{U}_v$ U_v/u_i
u, v components of velocity in x and y directions [m s^{-1}]
u_i the largest velocity in the system (if $u_\infty > v_p$, $u_i = u_\infty$; if $v_p > u_\infty$, $u_i = v_p$) [m s^{-1}]
u_s x component of the interfacial velocity [m s^{-1}]
u_∞ free-stream velocity [m s^{-1}]
$\bar{u}_s$ dimensionless x component of the interfacial velocity, u_s/u_i
$\bar{u}_\infty$ dimensionless free-stream velocity, u_∞/u_i
v_p plate velocity [m s^{-1}]
$\bar{v}_p$ dimensionless plate velocity, v_p/u_i
w_s mass flow per unit area [kg m^{-2} s^{-1}]
x, y streamwise and vertical coordinates [m]
y_l vertical position above vapor layer, $y-\delta_v$ [m]
Z density–viscosity product ratio, $\rho_l\mu_l/\rho_v\mu_v$.

Greek symbols

α $(n_v+1)(n_v+2)$
β subcooling parameter, $Pr_v c_{pl}(T_s-T_\infty)/Pr_l c_{pv}(T_p-T_s)$
γ ratio of boundary-layer thicknesses, δ_v/δ
Δ thermal boundary-layer thickness in liquid [m]
δ velocity boundary-layer thickness in liquid [m]
δ_v vapor-layer thickness [m]
$\varepsilon_m, \varepsilon_h$ eddy diffusivity of momentum and heat, respectively [m^2 s^{-1}]
$\varepsilon_p, \varepsilon_s$ plate and interface emissivities
ε_m^+ dimensionless eddy diffusivity of momentum, $\varepsilon_m^+ = \varepsilon_m/\nu$
η similarity variable defined by equation (10)
θ_l dimensionless liquid temperature, $\theta_l = (T_l-T_\infty)/(T_s-T_\infty)$
θ_v dimensionless vapor temperature, $\theta_v = (T_v-T_s)/(T_p-T_s)$
λ constant defined as $(\bar{v}_p+n_v\bar{u}_s)/(n_v+1)$
μ dynamic viscosity [kg m^{-1} s^{-1}]
ν kinematic viscosity [m^2 s^{-1}]
ρ mass density [kg m^{-3}]
σ Stefan–Boltzman constant, 5.67×10^{-8} W m^{-2} K^{-4}
τ shear stress [N m^{-2}]
φ parameter defined by equation (44)
Ψ stream function defined by equation (11)
ω parameter defined by equation (38).

Subscripts

av average
j for vapor layer j = v and for liquid layer j = l
l liquid
p plate
s vapor–liquid interface
v vapor
∞ liquid free stream.

Wang and Shi [14] developed a semi-empirical model to analyze forced flow turbulent film boiling of subcooled liquid along a horizontal stationary plate. Assuming a uniform velocity distribution and an expression for the eddy diffusivity of heat (ε_h) in the liquid layer (for $Pr_t \approx 1$, $\varepsilon_h = \varepsilon_m$), they solved a simplified form of the energy equation. The flow in the vapor layer was assumed to be the same as that of single-phase turbulent flow over a flat plate. Using the analogy between momentum and heat transfer and neglecting radiation and evaporative heat transfer, the wall heat flux and heat flux absorbed by the subcooled liquid were equated. Heat transfer results were presented in terms of a local Nusselt number based on the degree of subcooling and the liquid thermal conductivity. In most of the other studies, Nu_x was based on the plate superheat and the vapor thermal conductivity. The model constants appearing in the expression for the eddy diffusivity of momentum were determined from experimental measurements.

In contrast to the work of Wang and Shi [14], Abdallah [15] assumed that velocity gradients exist in the liquid, not in the vapor, layer. Assuming highly subcooled liquid and a large liquid velocity, existence of the vapor layer was neglected, rendering the interfacial velocity zero, and heat was transferred by single-phase convection. For a prescribed momentum eddy diffusivity model and power-law profiles for the liquid velocity and temperature, the integral forms of the momentum and energy equations were solved and local Nusselt numbers were calculated.

The review paper by Wang *et al.* [16] deals with both external and internal flow film boiling, including geometries such as a flat plate, circular tube, and rectangular duct. Both laminar and turbulent film boiling are considered. Also, a theory for high velocity flow film boiling heat transfer, which considers effects of subcooling and liquid velocity, is proposed.

From the foregoing survey, it is evident that most of the existing literature deals with either laminar film boiling or turbulent film boiling under highly subcooled conditions. Also, all of the turbulent film boiling studies are for flow over a stationary plate. Hence, objectives of this study are: (i) to obtain a local similarity solution for turbulent film boiling over a plate which is concurrently moving faster or slower than the free stream, (ii) to obtain an integral solution of the same problem, (iii) to determine the accuracy of the integral method by comparing results from the two solutions, and (iv) to obtain an improved understanding of related physical phenomena.

THEORETICAL ANALYSIS

Physical model and assumptions

The physical system under consideration is illustrated in Fig. 1. An x–y coordinate system is fixed at the exit of a die slot, and a continuous surface at uniform temperature T_p moves with a constant velocity v_p in parallel flow relative to a liquid stream. If the time elapsed from the moment of start-up is sufficiently long, the problem can be considered as steady with respect to the fixed coordinate system. It is assumed that (i) the plate temperature T_p is high enough for film boiling to occur and a stable vapor layer to form between the plate and a stable liquid layer; (ii) the liquid layer and plate move concurrently at different velocities; (iii) the liquid–vapor interface is smooth; (iv) the interfacial velocity is constant; (v) thermophysical properties are constant and evaluated at the film temperature, $T_{fv} = (T_p + T_s)/2$ and $T_{fl} = (T_s + T_\infty)/2$; (vi) vapor formation and the liquid boundary layer start at $x = 0$; (vii) the surface is impermeable and smooth; (viii) the body force is negligible compared to viscous and inertial forces, and (ix) the effect of radiation on vapor-layer formation is negligible.

Although the criterion for transition from a smooth to a rough-wavy vapor–liquid interface is unknown, certain characteristics of the interface are understood. For example, because the vapor–liquid interface is unsteady (wavy), vaporization occurs in a region of finite thickness [17], where vapor bubbles and liquid coexist. The thickness of this region depends on the subcooling and the free-stream velocity of the liquid. Under subcooled, forced convection conditions, vapor bubbles formed in this region are very quickly condensed by the subcooled liquid stream, contributing to a reduction in the thickness of the mixing region, a decrease in the magnitude of the oscillations,

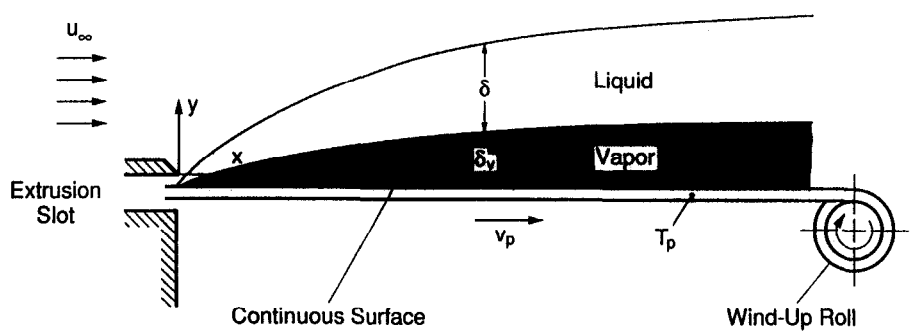

FIG. 1. Schematic of the physical model and coordinate system.

and hence a smoother interface. The net effect is to inhibit vapor-layer growth. With increased subcooling, the thickness of this region approaches zero and a smooth vapor–liquid interface is achieved.

High-speed motion pictures [3] of forced laminar film boiling along a hemispherically capped cylinder are consistent with the foregoing behavior. Large rates of vapor generation for a nearly saturated liquid induced intense mixing in the vapor–liquid region. As described by the authors of ref. [3], the interface was significantly disrupted by large rates of vapor generation and the tendency for the vapor to "escape" from the interface. For moderate liquid subcooling (11–28°C), the interface was relatively stable and free of the disruptions characteristic of temperatures near saturation. However, if the subcooling was increased further, interface instabilities were again observed and were attributed to a thinning of the vapor layer relative to the mean surface roughness. Generally, if the heater surface is smooth, any increase in the level of subcooling produces a more stable interface.

It is therefore concluded that the assumption of a smooth vapor–liquid interface is justified for subcooled conditions. However, because of the effect that surface roughness has on promoting interface disturbances for a thinning vapor layer [3], this assumption is tied to that of a smooth plate surface.

The current analysis employs a well-established two-phase boundary-layer approach for a subcooled liquid flow and a smooth interface moving at a constant velocity [4, 7–11]. Under these circumstances an analogy may be drawn between liquid flow over the vapor–liquid interface and single-phase flow over a moving surface. An eddy viscosity model associated with single-phase flow is therefore used in the present model.

For turbulent, incompressible, two-dimensional turbulent flow with no pressure gradient, the boundary-layer equations are

$$\frac{\partial u_j}{\partial x}+\frac{\partial v_j}{\partial y}=0 \tag{1}$$

$$u_j\frac{\partial u_j}{\partial x}+v_j\frac{\partial u_j}{\partial y}=\frac{\partial}{\partial y}\left[\left(\nu_j+\varepsilon_{mj}\right)\frac{\partial u_j}{\partial y}\right] \tag{2}$$

$$u_j\frac{\partial T_j}{\partial x}+v_j\frac{\partial T_j}{\partial y}=\frac{\partial}{\partial y}\left[\left(\frac{\nu_j}{Pr_j}+\frac{\varepsilon_{mj}}{Pr_{tj}}\right)\frac{\partial T_j}{\partial y}\right] \tag{3}$$

where j = v and j = l for the vapor layer and the liquid layers, respectively.

Solutions to the conservation equations are subject to boundary conditions at the plate surface, the vapor–liquid interface and at the edges of the liquid velocity and thermal boundary layers. The boundary conditions are given by

$$u_v=v_p,\quad v_v=0,\quad T_v=T_p\quad \text{at } y=0 \tag{4}$$

$$u_v=u_l=u_s,\quad T_v=T_l=T_s\quad \text{at } y=\delta_v \tag{5}$$

and

$$u_l=u_\infty,\quad T_l=T_\infty\quad \text{as } y\to\infty. \tag{6}$$

Mass, force and energy balances at the vapor–liquid interface ($y=\delta_v$) complete the description of the problem. Conservation of mass at the interface is expressed as

$$w_s=\rho_v\left(u_v\frac{d\delta_v}{dx}-v_v\right)=\rho_l\left(u_l\frac{d\delta_v}{dx}-v_l\right) \tag{7}$$

and force balance is given by

$$\tau_{yx|y=\delta_v}=\tau_{yx|y_l=0}. \tag{8}$$

The interfacial energy balance can be written as

$$q''_{y|y=\delta_v}+q''_R=q''_{y|y_l=0}+w_s h_{fg}. \tag{9}$$

The left-hand side of equation (9) represents the total heat flux arriving at the vapor–liquid interface, where the first term represents the conduction heat flux on the vapor side of the interface and second term represents the radiation heat flux (neglected in the analysis). The first term on the right-hand side of the equation represents heat transfer by conduction into the subcooled liquid, and the second term denotes the evaporative heat flux.

Local similarity solution

A solution of the model equations can be obtained using a similarity transformation. We introduce similarity and dimensionless variables which simplify the set of partial-differential equations. The similarity variables for the vapor and liquid layers are defined as

$$\eta_v=y\sqrt{u_i/\nu_v x}\quad\text{and}\quad \eta_l=(y-\delta_v)\sqrt{u_i/\nu_l x} \tag{10}$$

where, for $u_\infty > v_p$, $u_i=u_\infty$, and, for $v_p > u_\infty$, $u_i=v_p$. In terms of the dimensionless stream function, f_j,

$$f_j(x,\eta_j)=\Psi_j/\sqrt{u_i\nu_j x} \tag{11}$$

the velocity components u_j and v_j can be expressed as

$$u_j=u_i f'_j(x,\eta_j)$$

and

$$v_j=1/2(u_i\nu_j/x)^{1/2}(\eta_j f'_j-f_j)-(u_i\nu_j x)^{1/2}\frac{\partial f_j}{\partial x}. \tag{12}$$

Introducing the similarity and dimensionless variables into the model equations (1)–(3), we obtain

$$(b_j f''_j)'+\tfrac{1}{2}f_j f''_j=x\left(f'_j\frac{\partial f''_j}{\partial x}-f''_j\frac{\partial f_j}{\partial x}\right) \tag{13}$$

$$(r_j\theta'_j)'+\tfrac{1}{2}f_j\theta'_j=x\left(f'_j\frac{\partial\theta'_j}{\partial x}-\theta'_j\frac{\partial f_j}{\partial x}\right). \tag{14}$$

The boundary conditions given by equations (4), (5) and (6) now become

$$f'_v(0)=v_p/u_i,\quad f_v(0)=0,\quad \theta_v(0)=1\quad\text{at }\eta_v=0 \tag{15}$$

$$f'_v(\eta_v)_s=f'_l(0)=u_s/u_i,\quad \theta_v(\eta_v)_s=0$$

$$\theta_l(0) = 1 \quad \text{at } \eta_l = 0 \tag{16}$$

$$f_l'(\infty) = u_\infty/u_i, \quad \theta_l(\infty) = 0 \quad \text{as } \eta_l \to \infty. \tag{17}$$

Similarly, assuming that $(\eta_v)_s \approx$ constant, the interface ($y = \delta_v$) compatibility conditions, equations (7), (8) and (9), become, respectively,

$$\left(f_l + 2x\frac{\partial f_l}{\partial x}\right)_s = Z^{-1/2}\left(f_v + 2x\frac{\partial f_v}{\partial x}\right)_s \tag{18}$$

$$(f_l'')_s = (1+\varepsilon_{mv}^+)Z^{-1/2}(f_v'')_s \tag{19}$$

$$\beta(\theta_l')_s Z^{1/2} - (\theta_v')_s = Pr_v\left(f_v - 2x\frac{\partial f_v}{\partial x}\right)_s \Big/ 2Ja. \tag{20}$$

The local skin friction coefficient is expressed as

$$C_{f,x} = \tau_{yx|y=0}/(1/2\rho_l u_i^2) = 2Z^{1/2}|f_v''(0)|\,Re_x^{-1/2}. \tag{21}$$

The local Nusselt number based on the plate superheat and vapor thermal conductivity is given by

$$Nu_x = \frac{q''x}{k_v(T_p - T_s)} = \frac{-k_v(\partial T/\partial y)_{y=0}x}{k_v(T_p - T_s)}$$

$$= \frac{\mu_l}{\mu_v} Z^{-1/2}(\theta_v')_0 Re_x^{1/2}. \tag{22}$$

Local similarity characterizes turbulent flow conditions such that the transformed equations are not ordinary differential equations in η, but also depend on x. Hence, the local similarity method [18] is believed to be the most appropriate way to obtain the solution of the boundary-layer equations.

The transformed governing equations (13) and (14) were solved numerically using the Cebeci and Bradshaw [18] algorithm, which was modified to accommodate the two-phase boundary layer and to account for surface motion. Velocities were non-dimensionalized by the larger velocity (v_p or u_∞), with the Reynolds number based on the larger velocity. Treating the turbulent boundary layer as a composite of inner and outer regions [19], analytic expressions for eddy diffusivities of momentum have been inferred from experimental data for each region. Continuity of the eddy viscosity in the boundary layer was used to estimate the point of transition from one region to another. That is, the expression for the eddy viscosity in the inner region was applied from the surface outward, until its value matched that for the outer region. The complete formulation, with all constants and factors, is presented by Cebeci and Smith [19].

The numerical method used to solve the foregoing equations was originally developed by Keller [20] and provides second-order accuracy with an arbitrary mesh size and large x-variations. As summarized by Cebeci and Bradshaw [18], the solution is effected by first reducing the equations to a first-order system and then using central differences to obtain algebraic equations which are linearized and may be written in matrix form. The solution of the linear system is obtained using the block-tridiagonal-elimination method.

By prescribing the dimensionless interface velocity, $\bar{u}_s$, and vapor-layer thickness, $(\eta_v)_s$, together with the parameters Pr_l, Pr_v, Ja and Z, the governing equations were solved subject to the prescribed boundary and interface conditions. The η-direction mesh used in the calculations was finer in the region of larger gradients ($h_1 = 0.001$ and $K = 1.226$), with the requirement that the ratio of any adjacent $\Delta\eta$ intervals be constant. Applying the local similarity method to laminar film boiling, the calculation procedure and the computer program were validated through comparison of the predictions with published results [13]. The Nusselt number was determined from the wall temperature gradients, and the subcooling parameter β was calculated from equation (20).

Integral solution

Conservation equations of mass, momentum and energy for both vapor and liquid, together with compatibility conditions at the vapor–liquid interface, were also solved using the integral method. In integral form, governing equations for vapor phase are of the form

$$w_s = \frac{d}{dx}\int_0^{\delta_v} \rho_v u_v \, dy \tag{23}$$

$$\frac{d}{dx}\int_0^{\delta_v} \rho_v u_v^2 \, dy - w_s u_s = \tau_{yx|y=\delta_v} - \tau_{yx|y=0} \tag{24}$$

$$\frac{d}{dx}\int_0^{\delta_v} \rho_v c_{pv} u_v (T_v - T_s)\, dy = q''_{v|y=0} - q''_{y|y=\delta_v}. \tag{25}$$

The momentum and energy balances for the liquid layer are

$$\frac{d}{dx}\int_0^{\delta} \rho_l u_l (u_\infty - u_l)\, dy_l + (u_\infty - u_s)w_s = \tau_{yx|y_l=0} \tag{26}$$

$$\frac{d}{dx}\int_0^{\Delta} \rho_l c_{pl} u_l (T_l - T_\infty)\, dy_l + c_{pl}(T_s - T_\infty)w_s = q''_{y|y_l=0}. \tag{27}$$

Velocity and temperature profiles in the vapor layer are approximated by

$$\frac{\bar{u}_v - \bar{v}_p}{\bar{u}_s - \bar{v}_p} = \left(\frac{y}{\delta_v}\right)^{1/n_v} \tag{28}$$

$$\theta_v = \frac{T_v - T_s}{T_p - T_s} = 1 - \left(\frac{y}{\delta_v}\right)^{1/n_v} \tag{29}$$

and in the liquid layer by

$$\frac{\bar{u}_l - \bar{u}_s}{\bar{u}_\infty - \bar{u}_s} = \left(\frac{y_l}{\delta}\right)^{1/n_l} \tag{30}$$

$$\theta_l = \frac{T_l - T_\infty}{T_s - T_\infty} = 1 - \left(\frac{y_l}{\Delta}\right)^{1/n_l}. \tag{31}$$

The use of different values of n in the vapor (n_v) and

liquid (n_l) layers allows for prescription of different velocity and temperature profiles. To account for the development of velocity and temperature profiles with increasing Reynolds number, the analysis is developed in terms of an arbitrary value of the exponent n, although $n = 7$ is widely used for turbulent flow [21]. Solution of equation (23) yields

$$w_s = u_i \rho_v \lambda \frac{d\delta_v}{dx} \tag{32}$$

where $u_i = u_\infty$ for $u_\infty > v_p$ and $u_i = v_p$ for $v_p > u_\infty$.

To solve equations (24) and (26), expressions are needed for the shear stress at the plate surface and the vapor–liquid interface. Assuming applicability of the Blasius formula [22] for turbulent flow, which is modified for the effect of plate motion, the shear stress at the wall ($y = 0$) becomes

$$\tau_{yx|y=0} = C_v \rho_v u_i^2 (\bar{U}_v)^2 \left(\frac{U_v \delta_v}{\nu_v}\right)^{-m_v}. \tag{33}$$

Similarly, the shear stress at the vapor–liquid interface ($y_l = 0$) is

$$\tau_{yx|y_l=0} = C_l \rho_l u_i^2 (\bar{U}_l)^2 \left(\frac{U_l \delta}{\nu_l}\right)^{-m_l}. \tag{34}$$

In equations (33) and (34) the constants C and m are given by

$$C_j = A_j^{-m_j n_j} \tag{35}$$

and

$$m_j = 2/(n_j + 1). \tag{36}$$

The constant A is provided in tabular form for different values of n [22].

Integrating equation (24) and employing the expression for w_s, from equation (32), we obtain

$$I = \tau_{yx|y=\delta_v} - \tau_{yx|y=0} = \rho_v u_i^2 \omega \frac{d\delta_v}{dx} \tag{37}$$

where

$$\omega = \frac{(2\bar{v}_p + n_v \bar{u}_s)(\bar{v}_p - \bar{u}_s)}{(n_v + 1)(n_v + 2)} = \frac{D_1}{\alpha}(\bar{v}_p - \bar{u}_s). \tag{38}$$

Substituting equations (33), (34) and (37) into the force balance at the interface, equation (8), yields

$$I = \left[C_l \rho_l \bar{U}_l^2 \left(\frac{U_l \delta}{\nu_l}\right)^{-m_l} - C_v \rho_v \bar{U}_v^2 \left(\frac{U_v \delta_v}{\nu_v}\right)^{-m_v} \right] u_i^2. \tag{39}$$

Applying the Reynolds analogy (modified to account for the effect of surface motion), the following expressions are obtained for the heat flux at the plate surface and vapor–liquid interface

$$q''_{y|y=0} = \rho_v c_{pv} (T_p - T_s) u_i \bar{U}_v C_v \left(\frac{U_v \delta_v}{\nu_v}\right)^{-m_v} Pr_v^{-p_v} \tag{40}$$

$$q''_{y|y_l=0} = \rho_l c_{pl} (T_s - T_\infty) u_i \bar{U}_l C_l \left(\frac{U_l \delta}{\nu_l}\right)^{-m_l} Pr_l^{-p_l}. \tag{41}$$

The exponent p depends on specific physical conditions and will subsequently be determined on the basis of obtaining a best fit to local similarity results.

Substituting equations (32), (40) and (41) into equation (9), it follows that

$$I = u_i^2 \left[C_v \rho_v \bar{U}_v \omega \, Pr_v^{1-p_v} \left(\frac{U_v \delta_v}{\nu_v}\right)^{-m_v} - \beta C_l \rho_l \bar{U}_l \omega \, Pr_l^{1-p_l} \left(\frac{U_l \delta}{\nu_l}\right)^{-m_l} \right] \Big/ \left(\frac{\lambda}{Ja} + \frac{D_1}{\alpha}\right) Pr_v. \tag{42}$$

Combining equations (39) and (42), it then follows that

$$\frac{\delta_v^{m_v}}{\delta^{m_l}} = \varphi \frac{C_v \rho_v \bar{U}_v^{1-m_v} \nu_v^{m_v}}{C_l \rho_l \bar{U}_l^{1-m_l} \nu_l^{m_l}} u_i^{m_l - m_v} \tag{43}$$

where

$$\varphi = \frac{\omega \, Pr_v^{1-p_v} + Pr_v \left(\frac{D_1}{\alpha} + \frac{\lambda}{Ja}\right) \bar{U}_v}{\omega \beta \, Pr_l^{1-p_l} + Pr_v \left(\frac{D_1}{\alpha} + \frac{\lambda}{Ja}\right) \bar{U}_l}. \tag{44}$$

From equation (26), we also obtain

$$C_l \bar{U}_l^{1-m_l} \left(\frac{u_i \delta}{\nu_l}\right)^{-m_l} = \frac{I}{\rho_l \omega u_i^2} + \frac{D_2}{\alpha} \frac{d\delta}{dx}. \tag{45}$$

The above expressions are valid for both the fully turbulent vapor layer and the viscous sublayer. The maximum vapor-layer thickness for which the linear velocity and temperature profiles remain valid may be determined from the following criterion:

$$Re_{\delta_v} = \delta_v U_v / \nu_v < A_v B^{(n+1)/n} \tag{46}$$

where values of $B = 10$ and $B = 12$ have been suggested by Hsu and Westwater [23] and Fung and Groeneveld [24], respectively. The dependence of the vapor-layer Reynolds number on the local liquid-layer Reynolds number is included through the parameter n.

If the thickness of the vapor layer, which is mainly influenced by the degree of subcooling, is larger than the thickness of the viscous sublayer, it is assumed that turbulent flow conditions exist in both the liquid and vapor layers ($n_v = n_l = n$, $m_v = m_l = m$, $C_v = C_l = C$ and $p_v = p_l = p$). Also, the ratio $\gamma = \delta_v/\delta$ is constant. For this condition, the boundary-layer thickness of the liquid layer (for turbulent conditions $\delta \approx \Delta$) is found to be

$$\frac{\delta}{x} = (\bar{U}_l)^c \left(\frac{(1+m)C}{\frac{D_2}{\alpha} + \frac{\rho_v}{\rho_l} \lambda \gamma} \right)^d Re_x^{-a} \tag{47}$$

and the ratio of the vapor-layer thickness to the liquid boundary-layer thickness is

$$\gamma = \frac{\delta_v}{\delta} = \left(\frac{\nu_v}{\nu_l}\right)\left(\frac{\bar{U}_v}{\bar{U}_l}\right)^{(1-m)/m}\left(\varphi\frac{\rho_v}{\rho_l}\right)^{1/m}. \quad (48)$$

The dimensionless interfacial velocity can be expressed as

$$\bar{U}_l = |\bar{u}_\infty - \bar{u}_s| = \frac{\bar{U}_v}{\varphi} + \frac{\alpha}{D_2}\left[\omega - \lambda\left(\bar{U}_l - \frac{\bar{U}_v}{\varphi}\right)\right] \times \frac{\mu_v}{\mu_l}\left(\varphi\frac{\rho_v}{\rho_l}\right)^{1/m}\left(\frac{\bar{U}_v}{\bar{U}_l}\right)^{1/(m-1)}. \quad (49)$$

The local skin friction coefficient reduces to

$$C_{f,x} = \tau_{yx|y=0}/[(1/2)\rho_l u_i^2] = 2C^d\frac{\bar{U}_l^{2d}}{\varphi}(1+m)^{-a}\left(\frac{D_2}{\alpha} + \frac{\rho_v}{\rho_l}\lambda\gamma\right)^a Re_x^{-a} \quad (50)$$

and the local Nusselt number based on the plate superheat and vapor thermal conductivity is

$$Nu_x = \frac{q''_{y|y=0}x}{k_v(T_p - T_s)} = C^d(1+m)^{-a}\frac{(\bar{U}_l)^c}{\varphi}\frac{\mu_l}{\mu_v} \times \left(\frac{D_2}{\alpha} + \frac{\rho_v}{\rho_l}\lambda\gamma\right)^a Re_x^d\, Pr_v^{1-p}. \quad (51)$$

If the liquid is highly subcooled, the vapor layer coincides with the viscous sublayer, and the vapor velocity and temperature profiles are nearly linear ($n_v = 1$, $m_v = 1$, $C_v = 1$ and $p_v = 1$). Since the shear stress at the plate equals the shear stress at the interface for a linear velocity profile, equation (37) yields $I = 0$. The foregoing expressions then become

$$\frac{\delta}{x} = (\bar{U}_l)^c\left[\left(1+m\right)C\frac{\alpha}{D_2}\right]^d Re_x^{-a} \quad (52)$$

$$\delta_v = C^{-1}\frac{\rho_v}{\rho_l}\left(\frac{\bar{U}_v}{\bar{U}_l}\right)^2\left(\frac{\bar{U}_l}{\nu_l}\right)^m\left(\frac{\nu_v}{\bar{U}_v}\right)u_i^{m-1}\delta^m \quad (53)$$

$$\bar{u}_s = \frac{\bar{u}_\infty + \beta(Pr_l)^{1-p}\bar{v}_p}{1+\beta(Pr_l)^{1-p}} \quad (54)$$

$$C_f, x = \tau_{yx|y=0}/[(1/2)\rho_l u_i^2] = 2C^d\frac{\bar{U}_l^{2d}}{\varphi}(1+m)^{-a}\left(\frac{D_2}{\alpha}\right)^a Re_x^{-a}. \quad (55)$$

The local Nusselt number based on the plate superheat and vapor thermal conductivity is given by

$$Nu_x = \frac{q''_{y|y=0}x}{k_v(T_p - T_s)} = C^d(1+m)^{-a}\beta(\bar{U}_l)^c\frac{\mu_l}{\mu_v}\left(\frac{D_2}{\alpha}\right)^a Re_x^d\, Pr_l^{1-p}. \quad (56)$$

When the difference between the free-stream and plate velocities is close to zero, as, for example, when the plate moves very slowly through a quiescent liquid or when a low-velocity liquid stream flows over a stationary plate, the foregoing model would predict vanishingly small heat transfer and skin friction (equations (50) and (51)). However, in practice, these quantities do not vanish. According to Klimenko [25], heat is transferred from the plate to the interface across a vapor stream which results from hydrostatic pressure differences generated by the bubble release process. Vapor flow induced in this way may be laminar or turbulent, and from experimental data for nine different liquids, including water, Klimenko [25] proposed the following criterion to estimate transition from laminar to turbulent flow:

$$Ar_{L_{cr}} = (gL_{cr}^3/\nu_v^2)[(\rho_l - \rho_v)/\rho_v] > 10^8. \quad (57)$$

The Archimedes number Ar represents the ratio of the product of inertia and hydrostatic pressure forces to the square of the viscous force. The effect of surface forces is considered through the critical wavelength for a two-dimensional instability, L_{cr}. Expressions for the Nusselt number under laminar and turbulent flow conditions, together with the expression for L_{cr}, are provided by Klimenko [25].

The effects of radiation

In applications involving large plate temperatures, heat transfer may be significantly underpredicted if radiation is neglected. In film boiling radiation provides an alternative path for heat transfer from the plate to the vapor–liquid interface, and, by increasing the thickness of the vapor layer, it reduces convective heat transfer [26]. Since a change in convective heat transfer affects the temperature distribution, and hence radiation in the vapor layer, there is clearly coupling between convective and radiative heat transfer in film boiling. Bromley [27] performed a first-order analysis to assess the contribution of radiation in laminar film boiling, while Sparrow [28] improved the analysis by considering emission and absorption in the vapor layer. Sparrow concluded that, for low to moderate pressure systems, the radiative properties of the vapor had little effect on heat transfer and a radiatively non-participating vapor layer could be assumed.

To estimate the contribution of radiation in turbulent film boiling, a procedure used by Zumbrunnen *et al.* [12] for saturated laminar film boiling was adopted. Saturated film boiling provides conditions for which the relative effect of radiation is the most pronounced. The average total heat transfer coefficient across the vapor is defined as $(h_T)_{av} = (h_c + h_R)_{av}$, where

$$h_{av} = \left(\int_0^L h\,dx\right)\Big/ L$$

and L is the total length of plate. The quantity $(h_c)_{av}$ represents the convective heat transfer coefficient in the presence of radiation across the vapor layer. For

a turbulent (power-law) temperature profile in the vapor, equation (40) yields $(h_c)_{av} \propto \delta_v^{-m}$. For saturated conditions, all of the heat is used for vapor generation, and it follows that

$$q''_{y|y=\delta_v} + q''_R = w_s h_{fg} = (h_T)_{av}(T_p - T_s). \quad (58)$$

Hence, since the vapor mass flow w_v is proportional to the vaporization rate w_s, equation (58) yields the proportionality, $w_v \propto (h_T)_{av}$. Moreover, since $w_v \propto \delta_v$, it follows that $(h_c)_{av} \propto [(h_T)_{av}]^{-m}$. Using this result and noting that $(h_c)_{av} = (h_{co})_{av}$ when $h_R = 0$, where $(h_{co})_{av}$ is the convective heat transfer coefficient without radiation, it follows that

$$\frac{(h_{co})_{av}}{(h_c)_{av}} = \left(\frac{(h_c)_{av} + (h_R)_{av}}{(h_{co})_{av}}\right)^m \quad (59)$$

or rearranging

$$[(h_{co})_{av}]^{1+m} = (h_c)_{av}[(h_c)_{av} + (h_R)_{av}]^m \quad (60)$$

For $m = 1$ (a linear temperature profile in the vapor), this expression reduces to that obtained by Zumbrunnen *et al.* [12] for laminar film boiling.

Assuming a radiatively non-participating vapor layer, radiant energy exchange between the opaque, diffuse-gray plate and the liquid–vapor interface may be modeled as exchange between two parallel planes, in which case the radiation heat transfer coefficient is given by

$$h_R = \left(\frac{1}{1/\varepsilon_s + 1/\varepsilon_p - 1}\right)\left(\frac{\sigma(T_p^4 - T_s^4)}{T_p - T_s}\right). \quad (61)$$

This approximation is justified because the vapor film in forced-convection film boiling is generally very thin and exhibits a weak dependence on the streamwise coordinate measured from the leading edge.

RESULTS AND DISCUSSION

Results for the vapor-layer thickness, dimensionless interfacial velocity and local Nusselt number have been computed and are reported for fixed values of $Pr_l = 2.7$, $Pr_v = 1$, $Ja = 0.44$, $\rho_v/\rho_l = 0.0005$ and $\mu_v/\mu_l = 0.05$. These parameters are characteristic of quenching processes with water as the coolant [1]. The results are obtained for wide ranges of the subcooling parameter and plate velocity, for both $u_\infty > v_p$ and $v_p > u_\infty$.

Vapor-layer thickness

In film boiling the vapor layer acts as both a lubricant and an insulator. Momentum and heat transfer characteristics are directly influenced by the thickness of the vapor layer, which, in turn, is a function of the degree of subcooling and the plate velocity. For $Re_x = 10^7$, the variation of the vapor-layer thickness with the subcooling parameter and the plate velocity

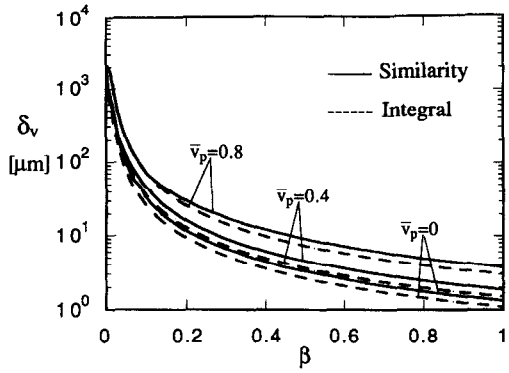

FIG. 2. Vapor-layer thickness for $Re_x = 10^7$.

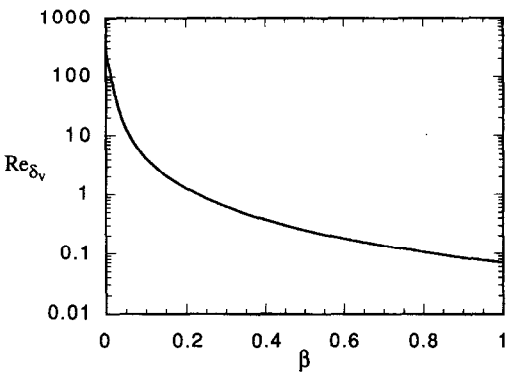

FIG. 3. Vapor-layer Reynolds number variation with β for $Re_x = 10^7$.

is shown in Fig. 2. For small β the vapor-layer thickness δ_v decreases rapidly with increasing β, while, for larger values of β, δ_v decreases more gradually, approaching zero (single-phase flow) as $\beta \to \infty$. Besides the well-known fact that both skin friction and heat transfer are inversely proportional to δ_v, it is important to stress that the vapor-layer thickness strongly influences the flow field. Under saturated conditions the vapor layer is sufficiently thick to encompass fully turbulent conditions. However, under subcooled conditions, this may not be the case, since the vapor layer is very thin. Even if the Reynolds number based on the streamwise coordinate and the kinematic viscosity of vapor suggests the existence of turbulent flow, the velocity and temperature are linear functions of distance from the wall. In other words, as also assumed by Gay [4], the vapor layer coincides with the viscous sublayer. In this case, even with a turbulent liquid layer, it is possible for the vapor layer to remain laminar.

For $Re_x = 10^7$ the variation of vapor-layer Reynolds number with β is given in Fig. 3, and the trend corresponds to that associated with dependence of the vapor-layer thickness on β. From equation (46) (with $B = 12$), it follows that, for $Re_{\delta_v} > 160$, turbulent conditions prevail in the vapor layer. From the results used to generate Fig. 3, such conditions would occur

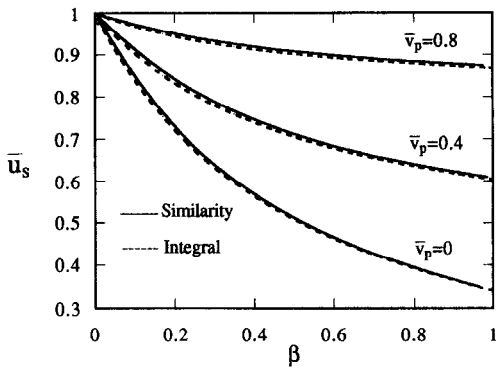

FIG. 4. Variation of the dimensionless interfacial velocity with β for $u_\infty > v_p$.

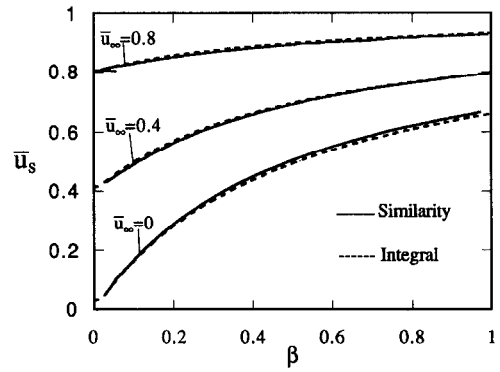

FIG. 5. Variation of the dimensionless interfacial velocity with β for $v_p > u_\infty$.

for $0 < \beta < 0.005$. This narrow β range, corresponding to near-saturation conditions, indicates that, in most quenching applications for which the liquid is highly subcooled [$(T_\infty \approx 20°C$, $T_p > 600°C)$ $0.05 < \beta < 0.2$], the vapor-layer thickness is of the same order as the thickness of the viscous sublayer.

Dimensionless interfacial velocity

The variation of the dimensionless interfacial velocity $\bar{u}_s$ with β is shown in Figs. 4 and 5 for $u_\infty > v_p$ and $v_p > u_\infty$, respectively. Similar trends have been obtained for laminar flow [13]. For $u_\infty > v_p$, the interfacial velocity decreases with increasing subcooling parameter and decreasing plate velocity, whereas for $v_p > u_\infty$ it increases with increasing β and $\bar{u}_\infty$. With increasing subcooling and $u_\infty > v_p$, the thickness of the vapor layer is reduced, bringing the interface closer to the plate. The corresponding increase in the drag force imposed by the plate decreases the interfacial velocity. If the plate velocity is increased, this effect becomes less severe and the interface velocity increases. The effect of increasing β on the vapor-layer thickness remains the same when $v_p > u_\infty$. However, with increasing β, the interface is further removed from the free stream, thereby decreasing its restraining influence on $\bar{u}_s$. Consistent with equation (54), the effect of increasing free-stream velocity on the interfacial velocity is similar to that of increasing plate velocity for $u_\infty > v_p$.

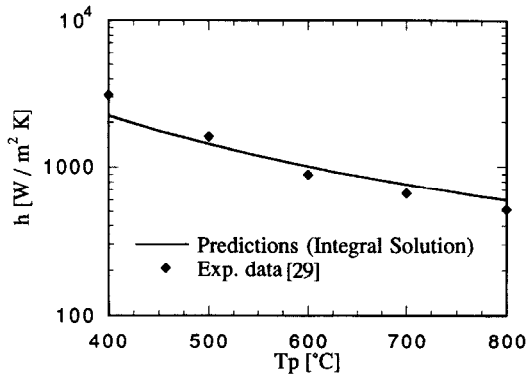

FIG. 6. Comparison of predicted local heat transfer coefficients with experimental results [29] ($T_\infty = 30°C$, $x = 0.4$ m, $u_\infty = 5.3$ m s^{-1}).

Heat transfer results

To assess the accuracy of the local similarity and integral methods, calculated results were compared with the experimental results of Otomo *et al.* [29], who measured local heat transfer on a stationary steel strip cooled by a planar water jet. Although the strip was stationary, the experiment was prototypic of situations for which the present film boiling model is applicable. The water bifurcated at the strip surface, dividing into two streams which moved along the strip until they collided with streams issuing from neighboring jets. Surface-cooling regimes included an impingement zone (using an expression given in [1], the zone width was estimated to be 10 mm), a film-boiling zone in parallel flow, and an interaction zone for neighboring jets. Jet momentum suppressed vapor-film formation in the impingement zone, but for large strip temperatures ($\sim 800°C$) a vapor film formed at the end of the impingement zone. Flow conditions in this region were turbulent, and a comparison of integral method predictions with the measured local convection heat transfer coefficient is made in Fig. 6. Since the half-width of the impingement zone (≈ 5 mm) is small compared with the location of the measurement (400 mm from the stagnation line), differences in upstream conditions at $x = 0$ (impinging jet in the measurements and $\delta = \delta_v = 0$ in the calculation) have a negligible effect on the comparison. The measurements were made in a transient experiment for which $T_\infty = 30°C$ and $u_\infty = 5.3$ m s^{-1}, and there is generally good agreement between the results. The largest discrepancy (about 30%) exists at the lowest plate temperature and may be due to the increased probability of liquid–plate contact, which would increase convective heat transfer coefficients relative to calculations based on the assumption of a continuous vapor blanket.

In order to improve agreement between Nusselt numbers predicted by the local similarity and integral

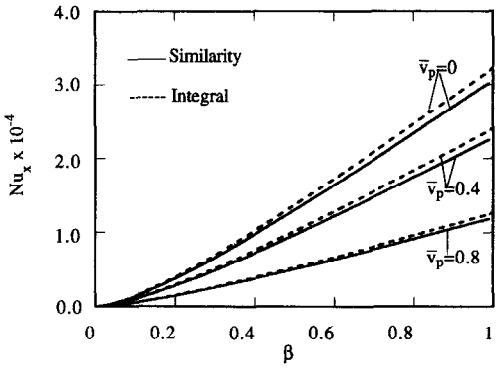

FIG. 7. Local Nusselt numbers for $Re_x = 5 \times 10^5$ ($u_\infty > v_p$).

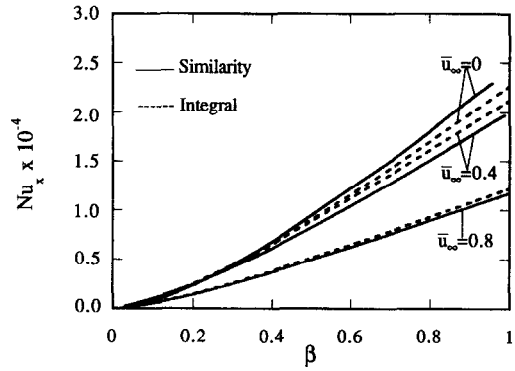

FIG. 10. Local Nusselt numbers for $Re_x = 5 \times 10^5$ ($v_p > u_\infty$).

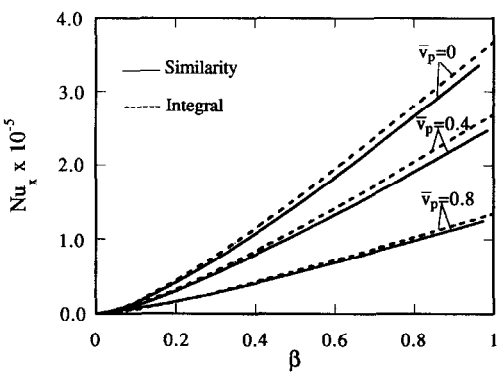

FIG. 8. Local Nusselt numbers for $Re_x = 10^7$ ($u_\infty > v_p$).

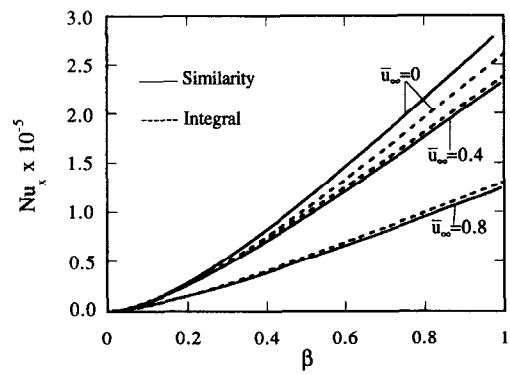

FIG. 11. Local Nusselt numbers for $Re_x = 10^7$ ($v_p > u_\infty$).

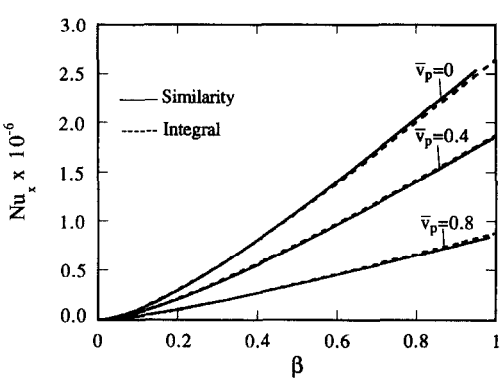

FIG. 9. Local Nusselt numbers for $Re_x = 10^8$ ($u_\infty > v_p$).

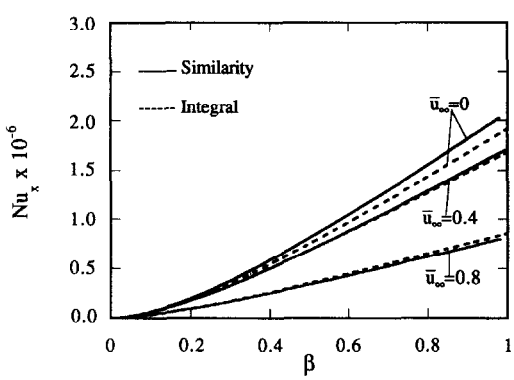

Fig. 12. Local Nusselt numbers for $Re_x = 10^8$ ($v_p > u_\infty$).

methods (Figs. 7–12), the value of the exponent n was changed from 7 ($Re_x = 5 \times 10^5$) to 8 ($Re_x = 1 \times 10^7$) and 10 ($Re_x = 1 \times 10^8$). These values were used for both $u_\infty > v_p$ and $v_p > u_\infty$. Although it was possible to achieve slightly better agreement by choosing a decimal value for the exponent n, restriction to integers was deemed to be appropriate for the purposes of this study. The best agreement between results associated with the local similarity and integral methods was obtained by using a value of $p = 1/3$ in equations (40) and (41). Hence the Prandtl number exponent $(1-p)$ appearing in the expression for the local Nusselt number, equation (51), equals 2/3, which is close to the value (0.6) suggested for single-phase turbulent flow over a flat plate [21].

Using the exponent n to account for development of the velocity and temperature profiles with increasing Reynolds number, good agreement was achieved between results for the local similarity and integral methods (Figs. 7–12). Due to the reduction in vapor-layer thickness with increased subcooling (Fig. 2), the local Nusselt number increases with increasing subcooling. In contrast to laminar film boiling over a moving surface, where the local Nusselt number

increases with increasing surface velocity [12, 13], the local Nusselt number decreases with increasing v_p in turbulent film boiling (Figs. 7, 8 and 9). Under subcooled, forced-flow conditions, heat is transferred mainly by convection at the vapor–liquid interface which, as already explained, may be viewed as a smooth surface moving at a constant velocity (u_s) through a liquid stream. As for laminar film boiling [12, 13], the interfacial velocity increases with increasing plate velocity v_p for $u_\infty > v_p$ (Fig. 4) and also increases with increasing free-stream velocity for $v_p > u_\infty$ (Fig. 5). Moreover, any reduction in the difference between free-stream and surface velocities (in the present case $\bar{u}_s$) leads to a reduction in both the velocity and thermal boundary-layer thicknesses of the liquid. For laminar flow, these reductions enhance skin friction and heat transfer. However, in turbulent flow, skin friction and heat transfer do not depend solely on the velocity and thermal liquid boundary-layer thicknesses, respectively, but through the turbulent viscosity and thermal conductivity, also depend on the difference between the free-stream and surface velocities [22]. Since this difference decreases with increasing surface velocity ($\bar{u}_s$), there is a reduction in the eddy transport coefficients and the effect exceeds that associated with the reduction in liquid boundary-layer thicknesses, causing the skin friction and heat transfer to decrease with increasing v_p. Mathematically, this behavior is represented by equations (50) and (51), where U_1 denotes the difference between the free-stream and surface velocities and D_2/α is the ratio of the liquid-layer-momentum (or enthalpy) thickness to the boundary-layer thickness.

Results obtained for Nu_x using the integral method (with $n = 7$) are in very good agreement with those of Gay [4], who assumed that under subcooled conditions, the vapor layer behaves as a thin viscous sublayer in a liquid flow (linear velocity and temperature profiles). Gay [4] also assumed $p = 2/3$. Based on results obtained using the local similarity method, it can be concluded that this assumption was quite realistic. In contrast to good agreement with the predictions of [4], Nu_x results obtained by Wang and Shi [14] and Abdallah [15] (in both cases very high subcooling was assumed) were larger than those of this study. Discrepancies are believed to be due to simplifications and inconsistencies associated with the previous studies [14, 15]. Wang and Shi [14] assumed the liquid-layer velocity profile to be uniform, and the interfacial velocity was taken to be equal to the free-stream velocity. As evident from Fig. 4, however, at large subcoolings the interfacial velocity is well below the free-stream velocity, but clearly does not vanish, as was assumed by Abdallah [15]. Moreover, the turbulent velocity distribution assumed for the vapor layer [14] is more likely to develop under saturated and not subcooled conditions. Namely, under highly subcooled conditions the vapor layer is suppressed and its thickness may be smaller than the thickness of the viscous sublayer, making development of a turbulent boundary layer impossible. Hence, the existence of a turbulent vapor velocity profile is inconsistent with some of the simplifications (negligible vaporization rate) related to the assumption of high subcooling.

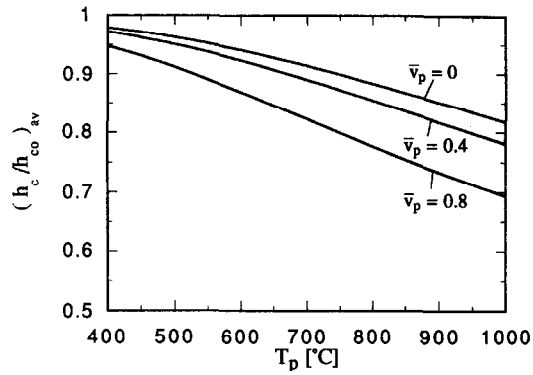

FIG. 13. Effect of radiation across the vapor layer on the average convective heat transfer coefficient for water with $\beta = 0$, $L = 0.5$ m, $u_\infty = 5$ m s^{-1}, $\varepsilon_p = 0.85$ and $\varepsilon_s = 1.0$.

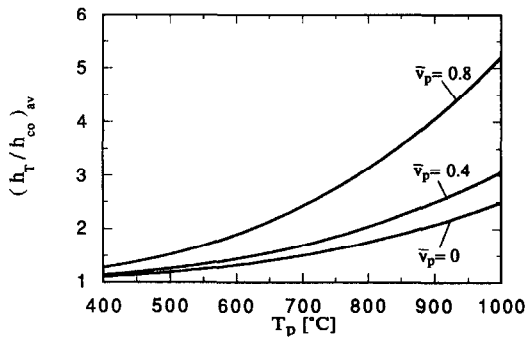

FIG. 14. Effect of radiation across the vapor layer on the average total heat transfer coefficient for water with $\beta = 0$, $L = 0.5$ m, $u_\infty = 5$ m s^{-1}, $\varepsilon_p = 0.85$ and $\varepsilon_s = 1.0$.

Radiation effects

Results obtained for the ratios $(h_c/h_{co})_{av}$ and $(h_T/h_{co})_{av}$ are given in Figs. 13 and 14. Figure 13 reveals that the value of h_c is less than that of h_{co}, and the ratio $(h_c/h_{co})_{av}$ decreases with increasing plate temperature. Also, because the reduction in h_c with increasing plate velocity is more pronounced than that of h_{co}, the ratio decreases with increasing v_p. Figure 13 shows that, for a stationary plate with $T_p = 1000$°C, the convective heat transfer coefficient is overpredicted by approximately 20% if radiation is neglected. However, the predictions of Zumbrunnen *et al.* [12] for laminar, saturated film boiling over a stationary plate at 1000°C reveal an overprediction of about 80%. The smaller overprediction for turbulent flow is attributed to the associated increase in convective heat transfer relative to radiative heat transfer. The foregoing comparison is only made for a stationary plate, since plate

motion has opposing effects on convective heat transfer in laminar and turbulent film boiling.

Figure 14 shows an increase in $(h_T/h_{co})_{av}$ with increasing plate temperature. This behavior, which reveals an increased contribution of radiation to the total heat transfer, represents the net effect of both increased radiation heat transfer and reduced convective heat transfer. Figure 14 reveals that, for a stationary plate with $T_p = 1000°C$, the total heat transfer coefficient is underpredicted by a factor of 2.5, if radiation is neglected. Laminar film boiling results [12] show that, for the same conditions, the underprediction is approximately seven-fold. Again, this difference for laminar and turbulent flows is attributed to the associated increase in turbulent convective heat transfer relative to radiative heat transfer. As already noted, since the plate motion reduces convective heat transfer in turbulent film boiling, the ratio $(h_T/h_{co})_{av}$ increases with an increase in v_p. From Figs. 13 and 14 we note that radiation plays an important role when the surface superheat is high and the degree of liquid subcooling is small. In such cases, radiation heat transfer should be included in determining a total heat transfer coefficient.

The effect of radiation on the vapor-layer thickness is more pronounced for saturated film boiling than for subcooled film boiling, where much of the heat transfer contributes to increasing the sensible energy of the subcooled liquid. For subcooled conditions, corresponding to a thin vapor layer (Fig. 2), convection dominates over radiation.

CONCLUSIONS

Results obtained by using local similarity and integral methods to solve the two-phase boundary-layer problem associated with subcooled turbulent film boiling are in good agreement, which could be improved by using non-integer values for the exponent n associated with the velocity and temperature profiles used in the integral solution. Moreover, the validity of the model is corroborated by agreement between model predictions and experimental results for the local Nusselt number.

Under subcooled conditions ($\beta > 0.005$), the thickness of the vapor layer is extremely small and the velocity and temperature profiles are nearly linear. Hence, since the subcooling parameter β is expected to be in the range between 0.05 and 0.2 for quenching processes with water ($T_\infty \approx 20°C$, $T_p > 600°C$), the simplified correlation for Nu_x (equation (56)) can be safely used. Results are presented in a manner that enables determination of heat transfer in terms of the subcooling parameter and the ratio of the flow to the plate velocity. However, application of the results requires knowledge of the critical Reynolds number for transition to turbulence in the liquid layer. Comparisons with additional experimental data (particularly for moving surfaces) would be desirable for further validation of the model.

Acknowledgement—This work was supported by the National Science Foundation under Grant CTS-9307232.

REFERENCES

1. J. Filipovic, R. Viskanta, F. P. Incropera and T. A. Veslocki, Thermal behavior of a moving steel strip cooled by an array of planar water jets, *Steel Res.* **63,** 438–446 (1992).
2. F. S. Gunnerson, and J. A. Meyer, An investigation of boiling behavior with applications to nuclear reactor safety, UCF Report No. 16-26-805 (1987).
3. W. S. Bradfield, R. O. Barkdoll and J. T. Byrne, Some effects of boiling on hydrodynamic drag, *Int. J. Heat Mass Transfer* **5,** 615–622 (1962).
4. A. Gay, Film boiling heat transfer and drag reduction, Convair Aerospace Division Report, San Diego, California, GDCA-DDB-71-001 (1973).
5. L. A. Bromley, N. R. Leroy and J. A. Robbers, Heat transfer in forced convection film boiling, *Indust. Engng Chem.* **45,** 2639–2646 (1953).
6. E. I. Motte and L. A. Bromley, Film boiling of flowing subcooled liquids, *Indust. Engng Chem.* **49,** 1921–1928 (1957).
7. R. D. Cess and E. M. Sparrow, Film boiling in a forced convection boundary layer flow, *ASME J. Heat Transfer* **83,** 370–376 (1961).
8. R. D. Cess and E. M. Sparrow, Subcooled forced convection film boiling on a flat plate, *ASME J. Heat Transfer* **83,** 377–379 (1961).
9. S. Ito and K. Nishikawa, Two-phase boundary layer treatment of forced convection film boiling, *Int. J. Heat and Mass Transfer* **9,** 117–130 (1966).
10. A. Nakayama and H. Koyama, Integral treatment of subcooled forced convection film boiling on a flat plate, *Wärme- und Stoffübertragung* **20,** 121–126 (1986).
11. P. R. Chappidi, F. S. Gunnerson and K. O. Pasamehmetoglu, A simple forced convection film boiling model, *Int. Commun. Heat Mass Transfer* **17,** 259–270 (1990).
12. D. A. Zumbrunnen, R. Viskanta and F. P. Incropera, The effect of surface motion on forced convection film boiling heat transfer, *ASME J. Heat Transfer* **111,** 760–766 (1989).
13. J. Filipovic, R. Viskanta and F. P. Incropera, Similarity solution for laminar film boiling over a moving isothermal surface, *Int. J. Heat Mass Transfer* **36,** 2957–2964 (1993).
14. B. X. Wang and D. H. Shi, A semi-empirical theory for forced-flow turbulent film boiling of subcooled liquid along a horizontal plate, *Int. J. Heat Mass Transfer* **28,** 1499–1504 (1985).
15. A. M. Abdallah, Analysis of turbulent-flow film boiling of a subcooled liquid over a horizontal plate, *Kerntechnik* **56,** 302–305 (1990).
16. B. Wang, D. Shi, X. Peng and J. Ma, Recent developments in flow film boiling heat transfer, *Prog. Natural Sci.* **2,** 481–490 (1992).
17. M. Cumo, Two-phase boundary layers in subcooled boiling, *Proceedings of NATO Advanced Study Institute 2, Istanbul, Turkey*, pp. 623–645 (1976).
18. T. Cebeci and P. Bradshaw, *Physical and Computational Aspects of Convective Heat Transfer*. Springer-Verlag, New York (1984).
19. T. Cebeci and A. M. O. Smith, *Analysis of Turbulent Boundary Layers*. Academic Press, New York (1974).
20. H. B. Keller, A new difference scheme for parabolic problems. In *Numerical Solution of Partial-Differential Equations* Vol. II (Edited by J. Bramble). Academic Press, New York (1970).
21. L. C. Burmeister, *Convective Heat Transfer*. John Wiley & Sons, New York, (1983).

22. H. Schlichting, *Boundary Layer Theory*. Pergamon Press, New York (1978).
23. Y. Y. Hsu and J. W. Westwater, Approximate theory for film boiling on vertical surfaces, *Chem. Engng Prog. Symp. Series* **30,** 15–24 (1960).
24. K. K. Fung and D. C. Groeneveld, A physical model of subcooled and low quality film boiling of water in vertical flow at atmospheric pressure, *Proceedings of the 7th International Heat Transfer Conference, Munich*, Vol. 4, pp. 381–386. Hemisphere, Washington, DC (1982).
25. V. V. Klimenko, Film boiling on a horizontal plate—new correlation, *Int. J. Heat Mass Transfer* **24,** 69–79 (1981).
26. J. Srinivasan and N. S. Rao, Numerical study of heat transfer in laminar film boiling by the finite-difference method, *Int. J. Heat Mass Transfer* **27,** 77–84 (1984).
27. L. A. Bromley, Heat transfer in stable film boiling, *Chem. Engng Prog.* **46,** 221–227 (1950).
28. E. M. Sparrow, The effect of radiation on film-boiling heat transfer, *Int. J. Heat Mass Transfer* **7,** 229–238 (1964).
29. A. Otomo, S. Yasunaga and R. Ishida, Cooling characteristic of steel sheet by water film in hot strip mill, *J. Iron Steel Inst. Japan* **73,** 996–1003 (1987).